Multiple Signal Representation Simulation of Photonic Devices, Systems, and Networks

Arthur Lowery, *Senior Member, IEEE*, Olaf Lenzmann, *Member, IEEE*, Igor Koltchanov, Rudi Moosburger, Ronald Freund, André Richter, Stefan Georgi, Dirk Breuer, and Harald Hamster

***Abstract*—Photonic systems design requires simulation over a wide range of scales; from wavelength-sized resonances in lasers and filters, to interactions in global networks. To design these global systems, while considering the effects of the smallest component, requires sophisticated simulation technology. We have developed the Photonic Transmission Design Suite, which includes five different signal representations, so that the details of device performance can be efficiently considered within a large network simulation. Alternatively, a design can be studied using a coarse signal representation before switching to a detailed representation for further refinement. We give examples of the application of these representations, and show how the representation of a signal is adapted as it propagates through a system to optimize simulation efficiency.**

***Index Terms*—Communication systems, data communication, design automation, intersymbol interference, optical amplifiers, optical crosstalk, optical fiber communication, optical propagation in nonlinear media, semiconductor lasers.**

I. Introduction

THE DESIGN of photonic systems has reached a stage in which simulation is no longer a luxury, but a necessity. This situation has developed over only a few years, because systems performance has reached a number of limits. Until the last decade, optical communications systems were chiefly limited by loss, dispersion, and transmitter and receiver performance [1]. However, loss is easy to calculate on the back of an envelope, and dispersion can be estimated by rule of thumb, aided by experience. It is the advent of optical amplifiers, enabling high powers and long unregenerated distances that have caused significant fiber nonlinearity that necessitated the use of numerical modeling: to calculate crosstalk caused by four-wave mixing and the interplay of nonlinearity and dispersion, such as in near-soliton and soliton systems [2]. In addition, long unregenerated systems suffer from polarization mode dispersion as a system limitation.

Furthermore, new problems requiring computer-aided design are beginning to come to light [3]. These problems include the design of components for dense wavelegnth-division multiplexing (WDM) systems, with several tens of channels. To continue an exponential growth in fiber capacity, *denser* WDM systems will be required as the fiber bandwidth is used up, which will have to operate with channel spacings reduced to a few times the channel bit rate [4]. These systems will require sophisticated modulation techniques, such as phase/amplitude/polarization modulation, perhaps including duobinary [5] or single-side band modulation [6]. Furthermore, the design of optical filters for wavelength multiplexers will have to become more sophisticated, because the filters will have to have flat passbands, good rejection, and low differential group delays (low dispersion). This design becomes problematic as the channel bandwidths become a significant fraction of channel spacing.

A push to all-photonic networks, or at least networks with photonic switching, will require careful consideration of optical crosstalk and multipath interference [7]. Low levels of crosstalk can have a significant effect because of the coherent mixing of optical fields. Even if the fields are from different transmitters, or carrying different data, or even from the same transmitter but over a ghost path longer by more than the coherence length of the laser, coherent mixing will cause large penalties. Thus, all paths should be considered in a photonic network, and this requires significant computation if all possible phase combinations are considered in networks with complex switch topologies [8].

All-photonic networks will require optical amplification to compensate for losses in switches and multiplexers on top of fiber losses. Cascades of amplifiers could cause power transients and strong interaction between WDM channels as the channels are switched on and off [9]. Transients are caused by the millisecond dynamics of the amplifiers, but they have nanosecond features, which is a difficult modeling problem because of the range of time scales. In the steady-state condition, the gain spectrum of amplifiers should be flattened to avoid large differences in signal-to-noise ratio (SNR) between channels [10].

Fig. 1 summarizes the challenges to modeling a photonic communications system, from transmitter, through add–drop multiplexers, optical cross connects, long-haul links, and, finally, at the receiver. The design of an optical component can directly and significantly affect the performance of an optical system. The system being affected could cost hundreds of millions of dollars: the component could cost tens of dollars. It would be too expensive to develop every component and optimize it by testing within a whole system. It would also take considerable time to optimize component designs by developing a series of prototypes. It may be impossible to

Manuscript received July 20, 1999; revised February 7, 2000. This work was supported in part by the European Union's ACTS DEMON Project.

A. Lowery is with Virtual Photonics Inc., Carlton 3053, Australia.

O. Lenzmann, I. Koltchanov, R. Moosburger, R. Freund, A. Richter, S. Georgi, and D. Breuer are with Virtual Photonics Inc., D10587 Berlin, Germany.

H. Hamster is with Virtual Photonics Inc., San Bruno, CA 94066 USA.

Publisher Item Identifier S 1077-260X(00)03856-9.

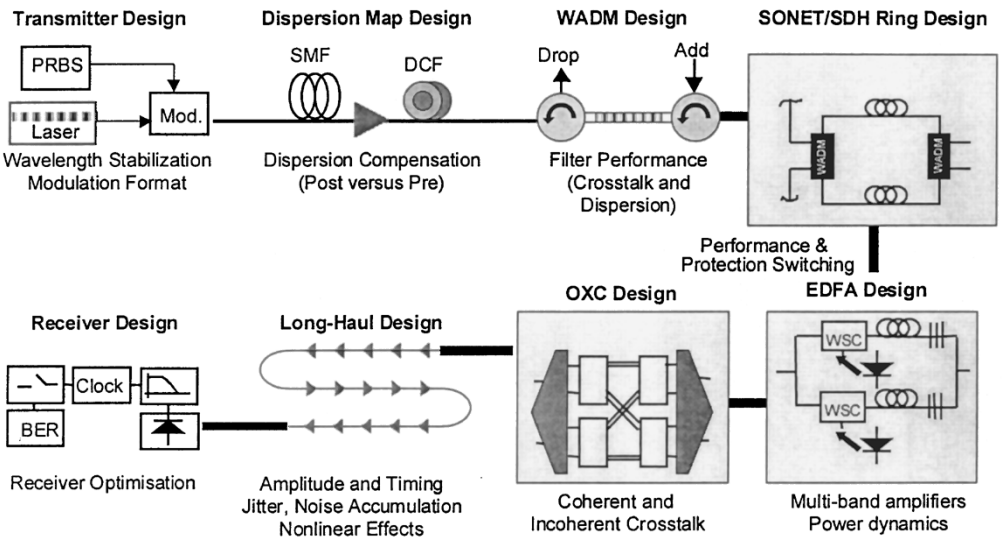

Fig. 1. Example of the modeling challenges within a photonic communications network.

compare component technologies not yet in mass production in large systems. However, the telecommunications industry is demanding rapid improvements and lower costs.

Because of the pressures of increased performance, increasingly sophisticated systems, and reduced design cycles, new design methods must be found [11]. One possibility would be to tightly specify the performance of each component to ensure the successful operation of the system as a whole. However, this process would lead to overly conservative design, which is not sustainable in a highly competitive industry. An attractive alternative is to employ computer-aided design and optimization to photonic systems and to replace the hardware prototype with software simulations. This replacement brings with it several advantages, not forgetting the ease of communicating and documenting software simulations.

This paper discusses the design philosophy that led to the development of a sophisticated photonic design automation (PDA) product [12], which is based on many tens of years of original research. The importance of having a wide range of signal representations is discussed in Section II. The provision of a range of models from abstract to physical is discussed in Section III. Examples of systems and network simulation are given in Section IV.

II. Signal Representations for Interconnecting Models

Photonic simulation is not new: over the years, many researchers, scientists, and engineers have developed numerical and semi-analytical models to solve particular problems. Groups of engineers have also worked on simulators for systems, for large design projects, such as transoceanic systems. What is new, however, is the recent emergence of commercial software for photonic simulation: first-generation commercial software focused on specific design problems, such as integrated optics and wave propagation. Second-generation tools allowed systems or components to be simulated using a single signal representation or simulation paradigm [13]. Third-generation tools provide flexible platforms for modeling at many scales of abstraction, from component to large network, each with the optimum simulation regime.

Third-generation tools require a mixture of signal representations, because it is often necessary to consider a component in a system in great detail, while treating the system or network more abstractly. Furthermore, in frequency space, it may be necessary to treat some WDM channels in great detail while only considering the *effect* of other channels on the channels under consideration. A further example, it is the separate treatment of signals and noise: the signal channels may occupy far less bandwidth than the noise from, say, an erbium-doped fiber amplifier (EDFA), but the noise can saturate other amplifiers or produce electrical noise on detection.

The key to developing a third-generation simulator, opposed to a solitary model, is to provide a flexible data interface representation between the modules [14]. Each module can represent a component or subsystem, but the key to a powerful and future-proof simulator is the ability for many modules to interact, providing novel solutions, or highlighting potential pitfalls in a design.

With this in mind, we have developed a flexible basis for treating signals and noise for our simulator photonic transmission design suite (PTDS). PTDS is based on the Ptolemy simulation engine [15], with a proprietary graphical user interface and proprietary signal representations. Furthermore, we have developed an extensive library of optical and electronic modules, covering many levels of abstraction. Ptolemy gives sophisticated control of the sequencing of modules during a simulation and provides a large library of communications and signal processing models. Its *tcl* scripting language [16] allows parameters to be specified as functions of higher level parameters or as random variables, which gives several powerful features as follows.

- Parameters can be made functions of global variables, such as a global filter bandwidth.
- Parameters can include any form of temperature sensitivity.

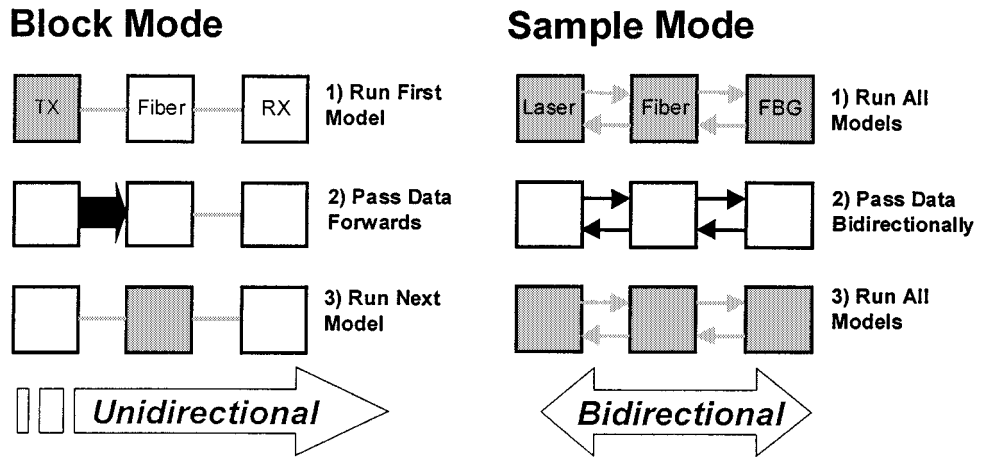

Fig. 2. Block and sample modes of simulation, showing unidirectional and bidirectional propagation and the firing sequence of modules.

- Parameters can be swept (using any functional form, from a central control) to analyze sensitivities.
- Parameters can be optimized automatically using iteration.

Two *modes* of simulation exist in PTDS: sample mode and block mode. Sample mode is for bidirectional simulation of closely coupled components, similar to that used in Optoelectronic, Photonic and Advanced Laser Simulator (OPALS) [11], but with a complex envelope signal representation for phase accuracy over the whole optical bandwidth. Block Mode passes data as arrays (blocks) of the complex envelope of the optical field, restricting bidirectionality to components spaced by more than a block length, such as optical switches separated by fibers, or to within a modules, such as in filters. The iteration schemes for block mode and sample mode are shown in Fig. 2. In block mode, the simulation progresses module by module. Usually, the module is run only once, with one block propagating from transmitter to receiver. However, multiple iteration can be performed, particularly if the system undergoes state changes, such as optical switching. The data within the blocks can be considered to be periodic or aperiodic. In the aperiodic case, the models remember their state from run to run, and linear convolution is performed in all filters. In periodic mode, the data within each block is considered to be independent, and circular convolution is used in the models.

In sample mode, modules communicate bidirectionally during iteration to simulate complex interactions and resonances between the components. Thus, every module must be fired to provide up-to-date information to its neighbors. Sample mode allows complex devices to be constructed from primitive components, such as mirrors, delays, gratings, and active region. It has been applied to many modeling problems, including high-speed, single-mode, Bragg-grating, stabilized and tunable lasers, picosecond pulse sources, clock regenerators, optical filter designs, and many more [17].

Sample mode has a single signal representation, covering all simulated optical frequencies and commonly assuming a single polarization. Block mode has both sampled and statistical signals, containing polarization information and center frequency, allowing a simulation to be partitioned spectrally into appropriate signal representations as follows.

- Sampled optical field signals, which contain full information from which optical and detected waveforms and spectra can be reconstructed. A single frequency band (SFB) can be used to cover all data channels (so that full interactions are calculated), or these can be represented individually using multiple frequency bands (MFB's), each with a center frequency and each covering one or more channels. MFB's, thus, can save on memory and computation when large unused gaps are in the spectrum.
- Statistical signals carrying average and deviations over the time-window of the block. Noise Bins (NB's) represent broad noise spectra efficiently as a mean power spectral density within a defined frequency range. NB's are effective for the amplified spontaneous emission (ASE) in an optical amplifier. Parameterized signals represent continuous wave (CW) signals or defined pulse shapes with mean power and jitter characteristics. They are useful for signal-to-noise calculations and to represent pumps or saturating signals in amplified systems. Noise generated within the spectral range of SFB or MFB signals can either be added to these signals or propagated separately as NB's.

In addition, PTDS passes logical information along a system, which can be used to identify the transmitter in a switched system, the modulation sequence, center frequency, and pulse shape (if applicable). Logical information is used in some forms of bit error rate (BER) estimation to compare transmitted and received sequences. BER's are estimated as follows:

- fitting distribution functions to received bit sequences, including noise, after they have been grouped into pattern sequences to isolate deterministic intersymbol interference from the stochastic noise [18];
- propagating noise and signal separately (using SFB/MFB and NB's) so that the noise statistics are presented deterministically to the receiver model [19]. This process neglects the interaction of noise and signal in nonlinear fibers, but it is deterministic.

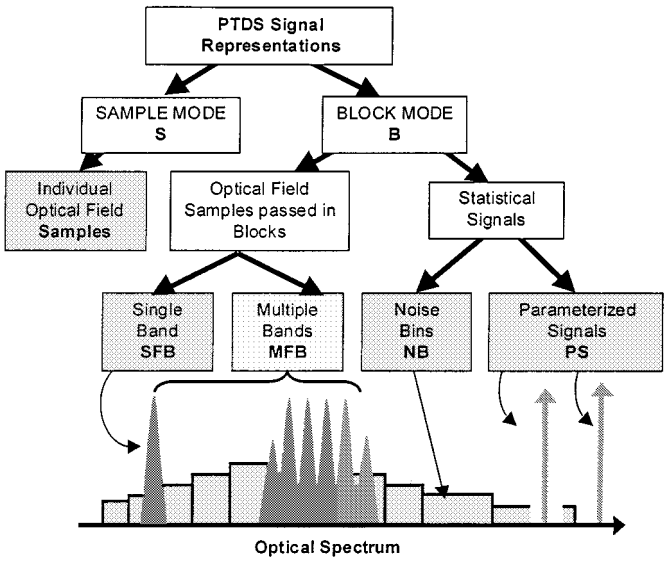

Fig. 3. Tree of simulation modes (sample, block) and signal representations. In block mode, the spectrum can be covered by four different signal representations for efficiency.

A. Conversion Between Signal Representations

Fig. 3 showed how the simulated spectrum can be divided into different block-mode signal representations according to optical frequency. A simulation can also be divided into different signal representations along its length, which implies conversion between representations along the signal path. This conversion can be done automatically or can be forced, using "nonphysical" modules. Furthermore, sampling rates can be changed, for example:

- to increase the simulation bandwidth, to accommodate four-wave mixing products during a nonlinear optical fiber simulation;
- to reduce data size when the optical or electrical bandwidths are reduced by filtering.

As an example of changing the signal representations along a system, Fig. 4(a) shows an optical amplifier schematic, with the signal representations annotated. The transmitters produce SFB's, each with a distinct carrier frequency. When multiplexed together, the SFB's become an MFB (a group of SFB's), although they will combine into a single band if their carriers overlap or if forced to. The pump laser adds a parameterized signal (PS), which feeds into a length of doped fiber. This produces wideband ASE in the form of NB. Noise within the sampled bands can be added to the bands or propagated separately.

Fig. 4(b) shows signal propagating through an amplified fiber system. Again, four SFB's are combined at the WDM coupler to form an MFB, and the EDFA puts all noise into NB's. In order to calculate the full interaction between all of the channels and the carriers and the noise, the fiber model first converts the MFB's and NB's (within the MFB spectral range) to a single-sampled band (SFB). This conversion allows for full nonlinear interaction between all signal channels and all noise within the signal sampled bands. The NB's outside the signal band will continue to propagate along the system.

The above examples show the *spatial* and *spectral* mapping of signal representations onto a system simulation. The type of

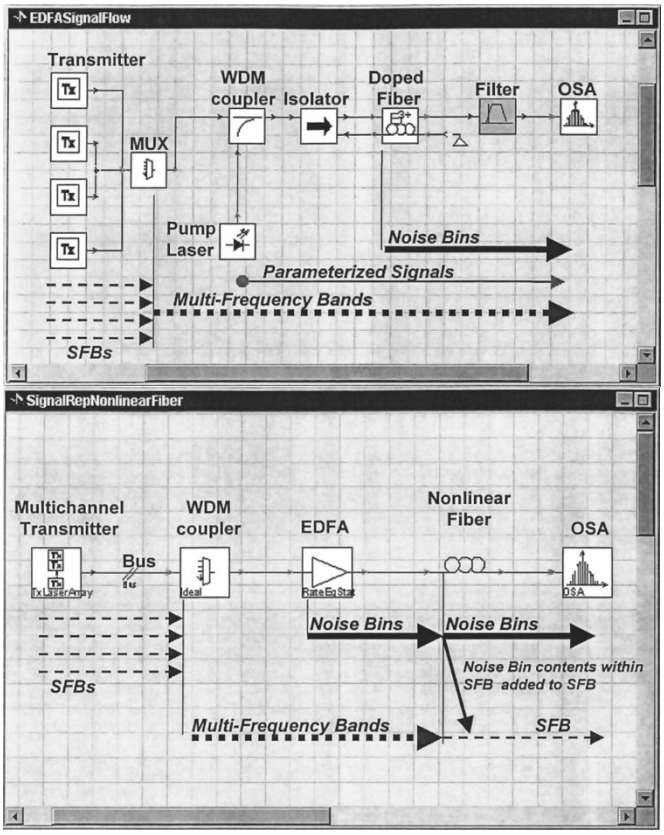

Fig. 4. Changing signal representations along a simulation. (a) Optical amplifier modeling with parameterized signals to represent pumps and (b) systems modeling with noise added to an SFB before nonlinearity calculations.

signal representation is controlled by the source modules, and it can be changed automatically (for example, when overlapping SFB's are combined in a multiplexer, they become a *single* SFB). Conversion modules are also provided between signal representations, including between block and sample modes. Global parameters can be used to choose signal representation, allowing coarse first-cut simulations, followed by detailed simulations. Also, network simulations tend to use the more abstract signal representations, whereas component modeling requires the sample mode to represent the interactions between closely spaced devices.

III. Model Abstraction

The simulation of photonic networks covers many scales of problem, from the details of the dynamics of quantum wells to interaction in fibers within global networks. It is therefore impossible to model a *complete* system on the scale of its smallest component; however, it is possible to vary the scale of the simulation from component to component. We have adopted a range of models for all but the most trivial of components. For example, our laser models range from CW sources with linewidth, through pulsed laser models, to single-mode-rate equations, to multisection wide-spectrum, large-signal transmission-line laser models (TLLM's). Our optical amplifier models are described by simple measured parameters, such as gain and noise, through frequency- and power-dependent external measurements, to full forward

TABLE I
COMPARISON OF SEMICONDUCTOR LASER MODELS

MODEL / FEATURE	CW Laser	Pulsed Laser	Rate Equation Laser	Transmission -Line Laser Model
Bidirectional				Yes
Linewidth	Yes	Yes	Yes	Yes
RIN/ASE	Can be added as a white-noise source	Can be added as a white-noise source	Yes	Full Spectra
Dynamics		Flat response	Calculated	Full
Chirp		Simplified Adiabatic and Dynamic forms	Adiabatic and Dynamic calculated numerically	Adiabatic, Static, SHB calculated numerically
Multimode	Can be cascaded to form multimode	Can be cascaded to form multimode		Yes (full spectrum)
Longitudinal Effects				Yes
External Feedback				Yes
DFB structure				Yes (incl. QWS, Gain Coupled)
Signal Representations	PS, NB, SFB, MFB, Sample Mode	PS, NB, SFB, MFB	PS, SFB, MFB,	Sample Mode

and backward simulation of an amplifier built from pumps, doped-fiber, and passive components. Our fiber models range from simple delays to frequency decomposition methods operating simultaneously on four signal representations, through split-step Fourier methods, to fast semi-analytical methods for ultrafast TDM/WDM systems.

A feature of PTDS is that most models select their algorithms automatically, depending on the signal representations they are given as inputs. Thus, *each* model contains a wide-range of abstractions. Where appropriate, the interactions between different representations will be considered. For example, an optical amplifier model made from individual components will process statistical representations of pumps and noise, together with multiple signals representing individual WDM channels. Examples are given below.

A. Optical Sources

The performance of the optical source can have a profound impact on the performance of a system. For example, it is well known that chirp in directly modulated lasers causes significant pulse broadening in dispersive fibers [20]. External modulators can be designed or driven to have zero chirp, or to have an optimized chirp. We have laser models from an abstract pure-sine wave at one end of the scale, to a full longitudinally inhomogeneous model at the other [21]. In between, the models assume single-modedness and homegeneity. The range of models is shown in Table I.

Note that dual mode lasers can be formed using two single-mode models to enable the effect of a single side mode on a system to be assessed. Furthermore, complex and novel laser designs can be studied by interconnecting separate sample mode laser models to form multicontact, multisection, multicavity lasers, such as grating stabilized lasers and tunable lasers. An example of a Bragg-Grating, stabilized laser design modeled in sample mode is given in Fig. 5 and is discussed in detail later.

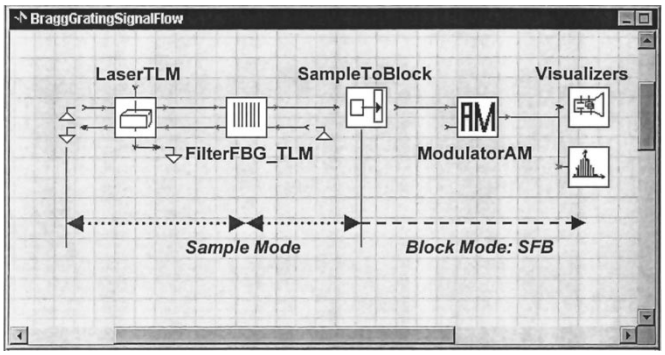

Fig. 5. Bragg grating, stabilized transmitter schematic, using sample mode to pass signals bidirectionally between two closely spaced components and block mode for the remainder of the simulation.

B. Optical Fibers

Although the Kerr nonlinearity in optical fibers is small, the use of extremely long fiber links, operated at high powers, means that the effect of the nonlinearity can be large and becomes a limiting factor in WDM systems. Nonlinearity leads to self-phase modulation within a channel, giving pulse shaping and the possibility of soliton systems. In WDM systems, it leads to crosstalk between channels and timing jitter caused by cross-phase modulation. Our fiber models are mostly based on the split-step method, in which the fiber is divided into sections. Within each section, the effects of dispersion and nonlinearity are treated separately [22]. The dispersion is treated in the

frequency domain as a frequency-dependent phase shift, and the nonlinearity in the time domain, as a phase shift dependent on instantaneous power. The step length is adaptable to give a maximum phase shift per step. Split-step models are provided for aperiodic or periodic boundary conditions.

For generality, all signal representations are converted into a single sampled signal, covering the whole wavelength range (Fiber NLS module). This conversion treats all interactions between the WDM channels. However, the independent channels, represented as MFB's can be calculated separately if the effects of four-wave mixing between the bands are negligible. This calculation can be useful for simulating the degradation of the central channels in a system because of FWM, without considering the minimal effect of the channels well away from those under consideration. The remaining channels are propagated as PS, so that they can saturate the gain of amplifiers along the link, and Raman effects can be quickly estimated using parameterized signals and semi-analytical techniques.

The NLS Frequency-decomposition module allows control of the modeling of nonlinear interactions between different frequency types. This module is useful for identifying the cause of degradation in a system. Interactions (excluding FWM) between PS, MFB's, and NB's can be controlled. In the general case, the contents of NB's and MFB's can be converted into an SFB at the beginning of the fiber to give all interactions. Propagating the noise independently of the signal to allows fast signal-to-noise analysis (though interactions between the noise and the signal are neglected, for example, modulation instability [23]).

For estimating the effect of polarization dispersion, the Random Birefringence PMD module propagates two polarizations represented by coupled, nonlinear Schrödinger equations. At each step of the split-step algorithm, the polarizations are scattered randomly on a Poincaré sphere, with a uniform distribution of polarizations [24]. This distribution will give an increase in pulse spreading, which tends to be proportional to the square-root of the propagation distance. The worst-case PMD can also be calculated by turning the random scattering off.

Future optical links and networks with speeds of 10 Gb/s and beyond are likely to be based on return-to-zero coding schemes because of their advantageous interplay between dispersion and fiber nonlinearities [25]. Here, two physical effects mainly determine the transmission performance. First, severe pulse-shape deviations in time and amplitude deveop from the impact of ASE noise introduced by optical inline amplifiers. Neglecting the nonlinear impact of noise onto signal propagation, pulse degradation caused by ASE noise can be derived analytically for any arbitrary-chirped optical pulse [26]. Second, nonbalanced frequency shifts caused by interchannel pulse collisions in WDM transmission systems result in additional timing jitter. Using the approach of elastic collisions [27], an expression for the timing jitter can be found for any arbitrary-chirped optical pulse, provided that the main energy of a pulse stays within a bit slot. These approximations are the basis of efficient semi-analytical estimation techniques used in PTDS. Compared with split-step methods, these modules achieve a reduction in computational time of two orders of magnitude.

The range of fiber models, at the time of writing, is summarized in Table II. It should be noted that the flexible signal representations in PTDS gives the ability to model at many degrees of abstraction and to include proprietary code using Matlab, Python, or C code. This option is useful for researchers and engineers working on specialist applications. Note the inclusion of a bidirectional fiber model, which is simply a time delay. This model is useful for constructing photonic circuits, such as filter networks, ring resonators, and mode-locked lasers.

C. Optical Amplifiers

Optical amplifiers can be treated with many degrees of abstraction, as shown in Table III. The simplest of models assume flat gain, whereas blackbox [28] models interpolate the gain spectrum from two measured spectra at two saturation powers, and a input–output saturation curve. The parameters for our blackbox model can also be precalculated using a detailed inhomogenous "Giles" EDFA model [29], perhaps of a multistage, multiply pumped amplifier, based on measurements of the gain and absorption cross sections of the fiber. We have also implemented a dynamic EDFA model based on [30] for millisecond transients in systems.

Semiconductor optical amplifiers are modeled using rate equations (assuming constant carrier density, implying an exponential power growth) [31], or longitudinally discretized models with full dynamics using the TLLM [32]. Most of the amplifier models operate in block mode, except for the TLLM, which is sample mode. It is impractical to formulate EDFA models with gain saturation in sample mode, as the average power in a signal would have to be obtained from a long average of the signal. In block mode, the contents of the block represent the signal over all time, as it is assumed by the amplifier to be periodic. This signal allows the state of saturation to be calculated from the input signal. An example of using blackbox amplifiers to equalize the signal-to-noise of a WDM signal propagating through a chain of saturated EDFA's is given later. Here, PS and NB's are used for efficiency.

D. Optical Filters

The performance of optical filters will become more critical as WDM channel spacing becomes denser and the bit rate per channel is increased. This process will require the evaluation of filter designs in systems models, as the filter's impulse response will dramatically affect intersymbol interference as the ratio of filter bandwidth to data rate is reduced [33].

Optical filters can be modeled from using ideal filter forms, measured characteristics, or using sample-mode (time-domain) models of filter lattices. Bragg gratings are modeled either from a frequency-domain transfer-matrix analysis [34] or a time-domain scattering-matrix analysis based on the TLLM. These analyses give identical results, but the frequency domain models have more sophisticated design rules to allow dispersion compensation or bandwidth to be specified directly. Also, the frequency-domain model will operate with periodic boundary conditions, allowing long impulse responses to be wrapped-around. This model is useful when modeling

TABLE II
COMPARISON OF OPTICAL FIBER MODELS

MODEL / FEATURE	Delay Samples	Non-Linear Schrodinger	NLS Frequency Decomposition	Random Birefringence PMD	Aperiodic Boundary Conditions	Semi-Analytical
Overview	Simple bidirectional delay for building resonators	A/Symmetric split-step algorithm operating on MFB/SFB, or Raman gain only for PS + NB. FWM only within each SFB.	Allows interaction between different frequency bands (MFB), and Parameterized Signals to be turned on or off to identify causes of degradation.	Coupled Non-linear Schr ödinger Eqns. solved for two independent polarizations by applying random scattering of polarization after each step.	Split-Step Method using recursive all-pass filters or overlap-add Fourier method to describe fiber dispersion.	Fast semi-analytical calculation of timing and amplitude jitter statistics of arbitrary chirped Return-to-Zero (RZ) pulses propagating in an optically amplified WDM system.
Attenuation		Function of wavelength	Function of wavelength	Function of wavelength	Function of wavelength (overlap-add)	Constant; compensated by periodically-spaced, noisy, flat gain amplifiers.
Dispersion		Yes	Yes	Yes	Yes	Yes
Kerr Nonlinearity		Yes	Yes (but FWM only within individual bands)	Yes	Yes	Yes
Raman Gain		Split-Step (semi-analytically for PS + NB)	Split-Step (semi-analytically for PS + NB)		Split-Step	
Polarization Dispersion		Single polarization	Single polarization	Yes (random birefringence/ fixed (worst case))	Single polarization	Single polarization
Signal Representations	Sample Mode, All Block Mode	Block Mode SFB, PS, NB (includes conversion from NB, and to PS)	Block Mode SFB, MFB, PS and NB (includes conversion from NB, and to PS)	Block Mode SFB/MFB. No interaction between separate bands in MFB. (PS, NB and MFB can be converted to SFB)	Sample Mode, (aperiodic) Block Mode	Parameterized Signals with Pulse-shape and Jitter (RZ only, any shape)

dispersion compensation in which the walk-off of the pulses is far longer than the modeled sequence.

Most filter modules operate on MFB/SFB signals, samples signals and NB's. NB's offer an efficient way of determining the response of a network by exciting the network with white optical noise (which is deterministic in the NB representation). Alternatively, testing with an impulse in SFB/MFB/sample mode and using a Fourier transform will reveal the spectral response of the network, including its group delay and phase characteristics.

E. Simulation Accuracy

It is important to be able to build a level of trust in the results of simulations. This trust has been obtained as follows.

- Comparing with other numerical models: PTDS has been developed from earlier products, such as BroadNeD (BNeD GmbH), GOLD, and OPALS (Virtual Photonics Pty Ltd.), and models at HHI (Germany), the Australian Photonics CRC, and at our partner universities. This development has allowed extensive checking against independently developed numerical models. OPALS, GOLD, and BroadNeD were themselves tested against experimental results and as part of European-wide projects, including the COST-240 project on measuring and modeling advanced photonic telecommunications devices and the ACTS DEMON project.
- Cross-checking numerical methods: PTDS contains two dynamic laser models compared in a simulation example, and several fiber models, all of which have been cross checked to prove their ranges of applicability.
- Amplifier and some laser models allow a choice of numerical techniques, with specified accuracy. Other models are based on techniques whose accuracy scales with computational effort (for example, the TLLM is based on physical equivalent circuit analog to the laser, whose inaccuracies are presented as well-understood "parasitics." Running at two different sampling rates identifies inaccuracies and their worst-case magnitude.)
- Standard regression tests are regularly and automatically run on the software to detect compilation errors. These tests are based on analytical results, where available.
- Comparison with published work: when developing applications examples, PTDS results are compared with experimental, numerical, and analytical published work.

TABLE III
COMPARISON OF OPTICAL AMPLIFIER MODELS

MODEL / FEATURE	System Model	Black-Box Amplifier	Static EDFA	Dynamic EDFA	Erbium Fiber	SOA Rate Equation	SOA TLLM
Bidirectional	No	No	Bidirectional internally	Yes	Yes	No	Yes
Control Loop Target	Gain Power Saturation	Gain Power Saturation	Uncontrolled	Uncontrolled	Not Applicable	Uncontrolled	Uncontrolled
Gain Spectrum	Flat	Interpolated from measured curves for any input spectrum	From files with gain and absorption cross-sections	From files with gain and absorption cross-sections	From files with gain and absorption cross-sections	Flat	Parabolic with carrier dependence
Noise Spectrum	Flat	From measured curves as Noise Figure or ASE	Non-flat, calculated from physical model	Non-flat, calculated from physical model	Non-flat, calculated from physical model	No	Parabolic with carrier dependence
Saturation	Spatially-resolved; Input or Output Saturation Power	Total Photons or Added Photons	Calculated from model: Caused by signal and ASE, (Frwd. Bkwd.)	Calculated from model: Caused by signal and ASE, (Frwd. Bkwd.)	Calculated from model: Caused by signal and ASE, (Frwd. Bkwd.)	Calculated from input signal	Calculated from input signal
Dynamics	No	Block to Block	No	Yes (from rate equations)	No	Yes (interband)	Yes (inter&intraband)
Longitudinal Effects	No	No (but implicit in the measurements)	Yes	Adiabatic approximation (flat inversion)	Yes	Adiabatic approximation (flat carrier density)	Carrier density and travelling photon intensities
Signal Representations	PS, NB, SFB, MFB, Sample Mode	PS, NB, SFB, MFB	PS, NB, SFB, MFB	PS, NB, SFB, MFB	PS, NB, SFB, MFB	PS, NB, SFB, MFB	Sample Mode

- Customer acceptance: Virtual Photonics, Inc. (VPI) has over 100 customers, may of whom have compared results from PTDS with their own numerical models before making a purchasing decision.

The propagation of errors along a system can be checked by monitoring waveforms, spectra, and power along a simulation, which is an excellent way to test numerical validity. For example, the optical spectrum shows the results of nonlinear interactions of carriers, and it is easy to see if these fall within the simulated bandwidth (indicating a valid simulation bandwidth), and whether they are expected frequencies or are spectrally broadened. Each component in a simulation can be made active or inactive to identify its effect.

IV. EXAMPLE APPLICATIONS

Hundreds of different designs and proprietary techniques are in photonics, and from our experience, PTDS is helpful in most cases to achieve greater understanding of an individual device, the performance of a device in a system, and the optimization of a system overall.

The following applications have been chosen to be illustrative of the range of problems that can be solved with PTDS. These examples do not include standard solutions of fiber nonlinearity, as these are well covered elsewhere; however, they do illustrate the power of the signal representations in speeding a design process. The examples are as follows:

- sample mode for transmitter (laser) design;
- PS for jitter estimation in long-haul RZ systems;
- combined PS and NB's for iterative signal-to-noise optimization in an amplified WDM system;
- SFB for dispersion map planning in a TDM system;
- PS and MFB's for assessing the performance and crosstalk in wavelength-converting cross connects;
- a comparison between split-step (SFB) and frequency-decomposition (MFB) fiber models for modeling short-pulse interaction caused by cross-phase modulation.

A. Semiconductor Laser Design (Sample Mode)

For long-haul communications, the goals for semiconductor laser design include the folling:

- high output power;
- single-mode spectrum, with better than 35-dB difference between the power in the main mode and a side mode;
- low-intensity noise, especially for analog or high-bit-rate systems;
- narrow spectral width under direct modulation (chirp);
- tunability, if possible;
- fast modulation response, if directly modulated, with low overshoot;
- low threshold current and high efficiency;
- temperature insensitivity.

Simulation using sophisticated models can be used to design lasers with optimized characteristics to design novel

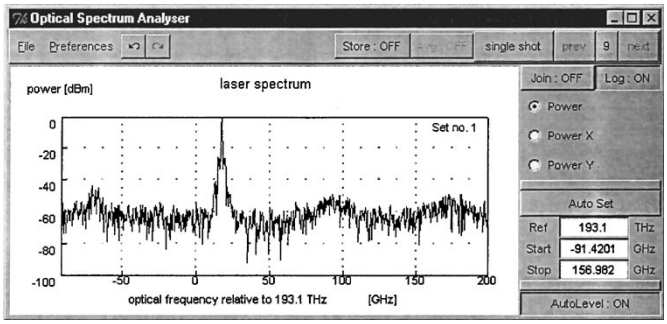

Fig. 6. Unmodulated optical spectrum of the Bragg grating, stabilized laser, showing the Bragg cavity modes within a dominant supermode, and the laser chip modes spaced at approximately 80 GHz.

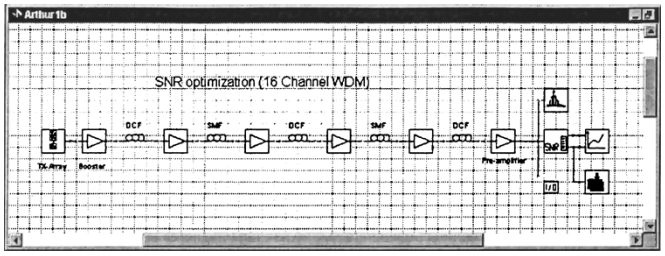

Fig. 7. Schematic of a multihop WDM system, in which the input powers are iteratively optimized to give equal channel SNR's.

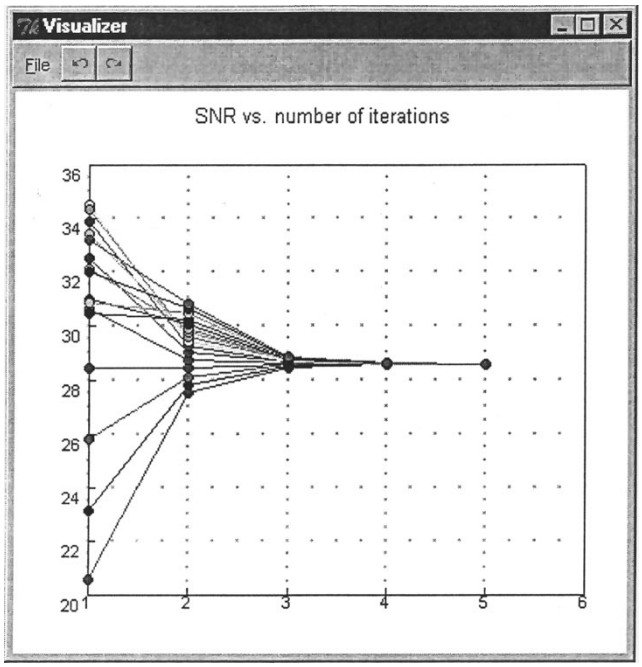

Fig. 8. SNR through five iterations of optimization, leading to equal signal to noise ratios.

lasers for specialist applications, or to identify the causes of performance imperfections in real devices. For these purposes, we have enhanced the TLLM [21], so that it can simulate over the broad spectral ranges required in WDM systems. The TLLM divides the laser into longitudinal sections, and then it propagate samples of the optical field between these sections, modifying the samples to represent stimulated and spontaneous emission, attenuation, reflections, and phase changes. The output of the module is a series of samples representing the optical waveform. All resonances of the cavity (including those from external components) are solved in the time domain, and the lasing spectrum can be found by Fourier transformation of the samples. The waveform also includes the dynamics of the laser, because the electronic processes are included into the laser model as rate equations.

The TLLM operates in sample mode, so that external components can interact with the laser by passing samples of the optical field back to the laser model at each iteration. This process allows complex lasers (tunable, multisection, multicontact, integrated mode-locked) to be built from interconnected models, and photonic circuits with active elements (wavelength converters, clock regenerators, limiters, photonic switches) to be simulated. A wide range of filters, couplers, delays, phase shifters, and modulators also operate in sample mode, allowing novel circuits to be designed.

As an example of the application of sample mode to circuit design, a semiconductor laser stabilized by a Bragg grating is simulated. The schematic is shown in Fig. 5 and comprises a laser module connected to a time-domain model of a Bragg grating (also based on TLLM techniques). The 1-cm Bragg grating reflects over a narrow stop-band, selecting one of the weak modes of the imperfectly (2%) antireflection-coated laser chip. The output of the laser is converted to block mode for efficient unidirectional propagation along the remainder of the system. Unfortunately, because of the long length of the compound cavity, several of the compound cavity's modes will lase, forming a supermode, as shown in Fig. 6. Weak resonances of the laser chip, because of imperfect antireflection coating, are also present. Many design parameters can be investigated using this simulation because of the close relationship between the model topology and the real device.

B. 10-Gb/s Amplified WDM System Signal-to-Noise Optimization (NB's and PS)

The optimum information-carrying performance of a long-haul saturated amplifier link is obtained when the SNR's is equalized over all channels. Fig. 7 shows the schematic of a 16-channel WDM system with a chain of six amplifiers, three sections of dispersion-compensating fiber (DCF), and two spans of single-mode fiber (SMF). The amplifiers have no gain equalization, so they suffer from a large spectral ripple. The object of this simulation is to optimize the input spectrum of the chain so that each WDM channel has the same SNR at the output of the chain, which gives the maximum information capacity for the link, but it is difficult to calculate as the gain spectrum of the amplifiers depends on their input powers. Thus, a self-consistent solution must be found iteratively. This process can be performed using a simple optimization loop, automatically included in the simulation using Ptolemy scripting language *tcl*.

For efficiency, the eye diagrams of each channel are not calculated during the optimization process. Rather, PS are used to represent the mean power in a WDM channel over a data sequence, and the NB's can be used to represent the noise in and around each channel. The EDFA models are able to calculate the saturation of the amplifier using a blackbox model [28], hence, the amplifier's gain spectrum from the input signals and noise. This model uses a simple, single-saturating wavelength measurement of an amplifier's gain to predict the gain for any set of input wavelengths and powers. Experimentally, we have shown excellent (within 0.5 dB) predictions of the gain of fully loaded WDM spectrum for a commercial amplifier [35], [36].

The output SNR's of the 16-channels, for the SNR optimization, for each iteration step are shown in Fig. 8. These channels converge in a few iterations. If the gain spectrum of the amplifiers were independent of the input power, the convergence would occur in an iteration step. The converged output spectrum is shown in Fig. 9. This figure shows a constant SNR (the PS are equal ratios above the NB's) for channels. Note that the NB's represent the noise within a 39-MHz range, whereas the SNR is calculated for a 0.1-nm bandwidth receiver, so the optical spectrum analyzer (OSA) display's SNR appears larger than it actually is. Also, the widths of the NB's have been automatically reduced around the ASE peak to maintain amplitude accuracy. This feature is designed to increase efficiency by optimizing the number of NB's covering the spectrum.

Once the SNR has been optimized, it is a simple task to switch the transmitters to give SFB signals so that the eye diagrams and bit-error rates (BER's) of the channels can be assessed. Similarly, multiple sweeps of the system can be performed, for example, to assess the performance of the system with one or more channels disabled.

C. 10-Gb/s Long-Haul System Design (Single Frequency Band)

The positioning of optical amplifiers in a long-haul system is a nontrivial problem because of fiber nonlinearities and the interplay between nonlinearities and dispersion. Amplifiers may be placed before sections of dispersive (single-mode, SMF) fiber, before sections of dispersion-compensating fiber (DCF), or both. The amplifier power will affect signal-to-noise, but less obviously, the shaping of the pulses by nonlinearities. The design is also affected by existing plant, such as installed fiber types, position of regenerator stations, and so on.

Fig. 10 shows a 10-Gb/s single-channel system to be optimized that includes alternate 80-km sections of single mode (SMF) and DCF to give 99.5% compensation, which was found to be optimum. The parameters for the fibers are given in Table IV. The transmitter is a zero-chirp external modulator, and the amplifiers include 1-nm filters. The receiver was assumed not to affect performance. The 128-bit sequences were simulated. Interestingly, the system has an initial length of SMF and the ability to set the output powers of the amplifiers. The design problem is to find the optimum amplifier output powers, and the best initial length of SM fiber to give the maximum transmission distance (that is, the maximum number of DCF–SMF spans). As Figs. 11 and 12 show, the initial length of SMF has a profound effect on the performance of the system,

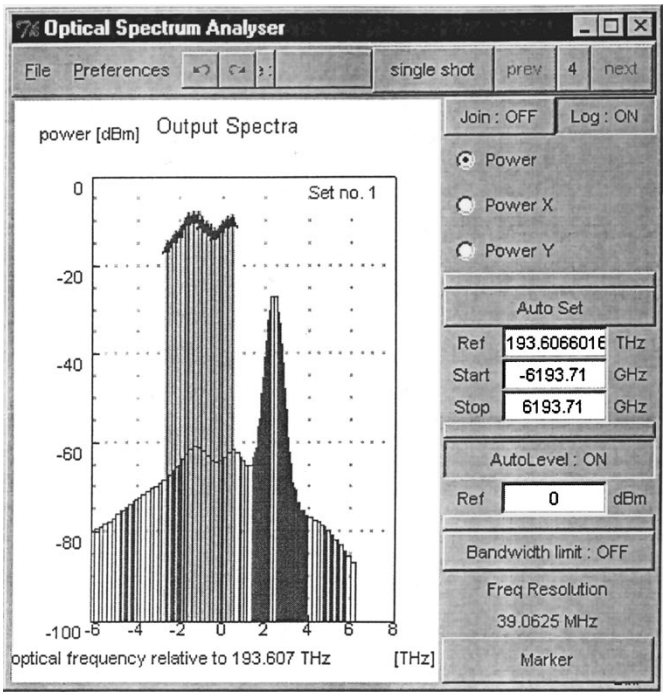

Fig. 9. Output spectrum after equalization for SNR. Note the noise bins (bars) are used to represent the ASE noise, whereas parameterized signals (arrows) represent the mean channel powers.

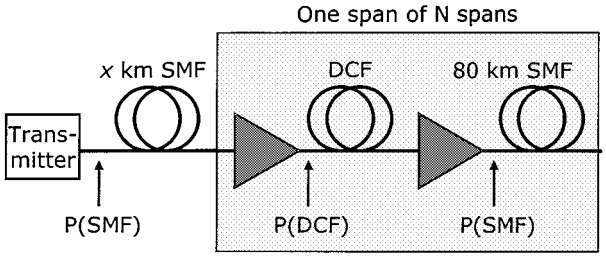

Fig. 10. Multihop dispersion-compensated system in which the input powers to the dispersion-compensating fiber (DCF) and the single-mode fiber (SMF) are adjusted for maximum transmission distance in number of spans.

and the optimum amplifier powers. The numbers of spans that can be covered are plotted as contours, for initial SMF lengths of 10 and 30 km. The 30-km system can operate over 60 spans for a Q of 6 by increasing the input power to the SMF, compared with the 10-km SMF case, which can only operate over 48 spans and requires lower amplifier output powers. Similar results, including experimental conformations using recirculating loop experiments, have recently been presented in [37].

D. Long-Haul WDM Return-to-Zero (RZ) Design—Estimation of Timing Jitter (PS)

Accumulated timing jitter due to interchannel pulse collisions and ASE-noise becomes the system limiting factor for RZ propagation over long-haul WDM links with bit rates of 10 Gb/s and beyond. This example illustrates semi-analytical techniques for

TABLE IV
FIBER PARAMETERS IN LONG-HAUL SIMULATION

FIBER	Single-Mode Fiber (SMF)	Dispersion-Compensating Fiber (DCF)	Unit
Length	80	12.5	km
Attenuation	0.25	0.5	dB/km
Dispersion	16.0	-102.0	$ps.nm^{-1}.km^{-1}$
Dispersion Slope	0.06	-0.2	$ps.nm^{-1}.km^{-2}$
Nonlinearity	2.6×10^{-20}	2.6×10^{-20}	$m^2.W^{-1}$
Effective Core Diameter	2.5×10^{-11}	7.0×10^{-12}	m^2

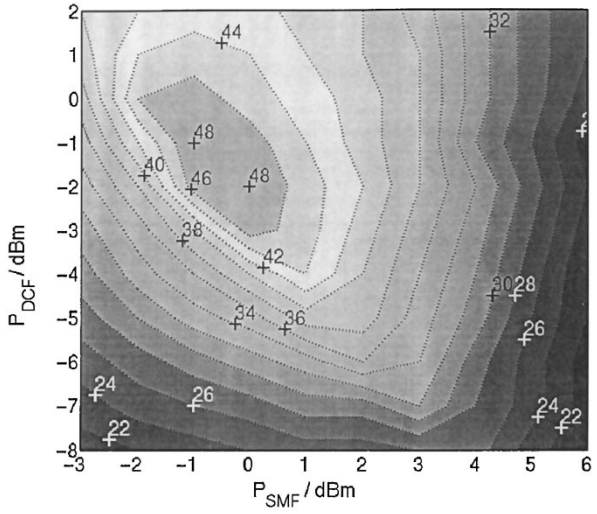

Fig. 11. Results of multiple simulations to determine the optimum input powers to the DCF and SMF. The labeled contours represent the number of hops that can be achieved for a particular combination of powers. The chart is for an initial length of SMF of 10 km.

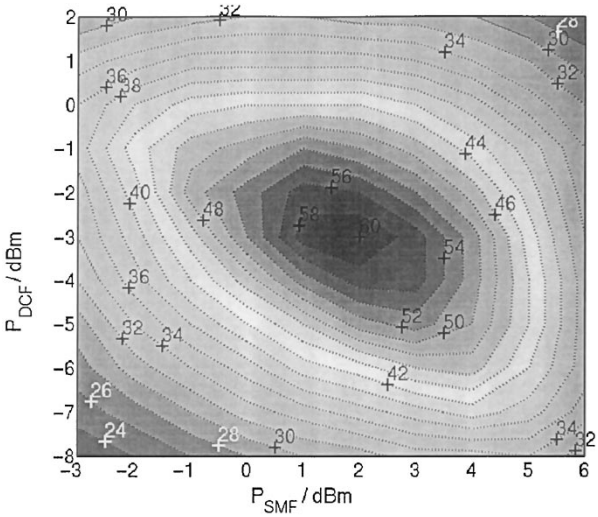

Fig. 12. Results of multiple simulations to determine the optimum input powers to the DCF and SMF. The chart is for an initial length of SMF of 30 km. Note the increased transmission distance that can be obtained over a short initial length of SMF.

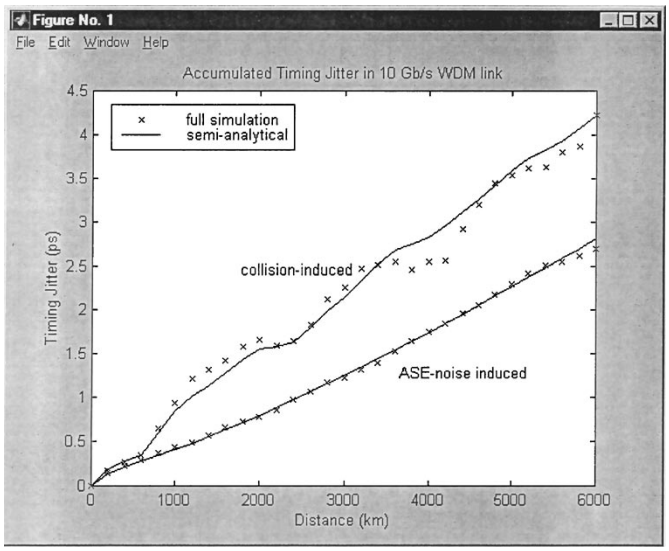

Fig. 13. Accumulated timing jitter of RZ propagation over an optically amplified WDM link at 10 Gb/s, using two modeling techniques.

calculating timing jitter. These techniques increase the computational efficiency by about two orders of magnitude compared with split-step simulations. Our example is a 10-channel WDM transmission system, using Gaussian pulses of 16.75 ps width at 10 Gb/s, and a dispersion managed fiber link. The length of the symmetrical dispersion map is 200 km; the average dispersion is 0.078 ps/nm-km. The amplifier spacing is set to 50 km, and each amplifier operates with a noise figure of 6.34 dB.

Fig. 13 shows the simulation results from the semi-analytical model in split-step models for collision-induced and ASE-induced jitter. The jitter for the split-step methods is estimated from 100 simulations by averaging the pulse time with respect to the same statistical propagation properties. Note that the modules performing the semi-analytical estimation techniques are operating with PS, and therefore pass data as modules as *average* pulse shapes and jitter values. This example shows that PS are efficient for optimizing long haul links with respect to amplifier spacing and positioning and to the applied dispersion map.

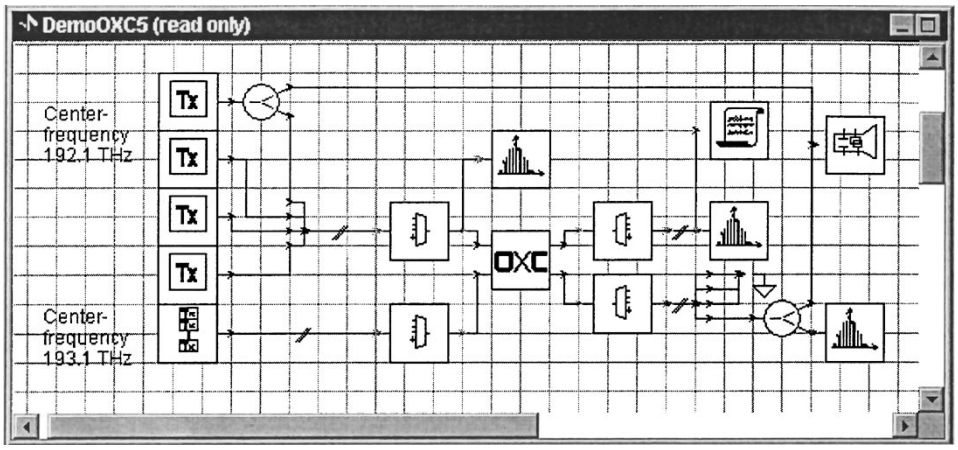

Fig. 14. Schematic to test the crosstalk performance of a wavelength-interchange, optical cross-connect, with two inputs each carrying four WDM channels. AWGM's are used to multiplex and demultiplex the test channels, and an text viewer (scroll icon) can display the signal powers in all possible signal paths for crosstalk analysis.

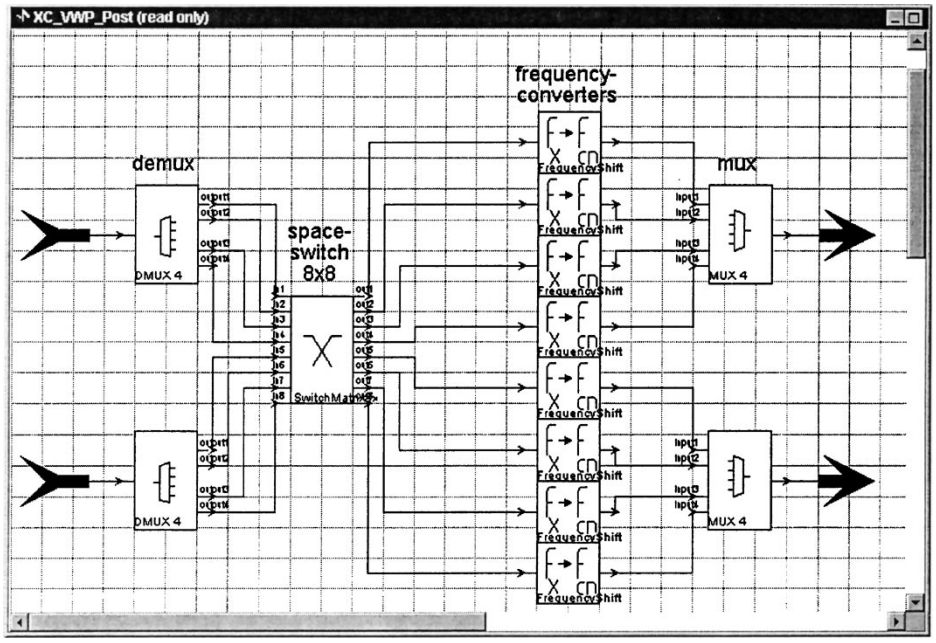

Fig. 15. Intenal configuration of the optical cross connect of Fig. 13, showing AWGM's for demultiplexing the WDM input channels, followed by a 8×8 space switch feeding into eight arbitrary, input-frequency, fixed-output frequency wavelength converters. Two AWGM's multiplex the outputs to two ports.

E. Crosstalk in WDM Network Design (MFB's and PS)

The increase in used bandwidth of optical fibers requires a similar increase in the capacity of interconnects. Photonic switching gives the possibility of building large-capacity switches. However, photonic switches may not offer the regeneration that is implicit in electronic switches, although wavelength converters offer some regeneration because of their nonlinearity. Photonic simulation can be used to assess the performance of optical cross connects within systems. Of particular interest is optical crosstalk, which can severely limit the number of optical interconnects in a system [38]. Many different technologies can be compared, including blocking, nonblocking, wavelength converting (using cross-gain, cross-phase, four-wave mixing, and optoelectronic technologies). In our example, we investigate the performance of an optical cross connect with two fiber inputs, each carrying four WDM channels (Fig. 14). The outputs are demultiplexed using arrayed-waveguide demultiplexers (AWG) [39]. The switch itself (Fig. 15) comprises AWG demultiplexers, an 8×8 space-switch (made from 1×8 distributors and 8×1 collectors), and eight fixed-output-frequency wavelength converters. The eight outputs are remultiplexed using AWG's to two output ports.

Fig. 16 shows the output spectra of the output of the top AWGM, created using MFB (sampled) signals. Ideally, one

dominant channel per frequency should exist. However, the effects of the space-switch crosstalk, imperfectly demultiplexing filters, imperfect AWGM filtering, imperfect wavelength conversion degrade the channels. Turning off transmitters or converters, or globally setting filter parameters, crosstalk amplitudes and phases, can identify these effects individually. To investigate coherent crosstalk, the simulation can be driven through a number of phase states using swept parameters, or random phase parameters. Fig. 17 shows the eye diagram of one switched and converted channel. This figure has slow-leading edges because of the transient response of the cross-phase wavelength converters and large fluctuations because of crosstalk in the wavelength converters because of imperfect input filtering.

The simulation can also be globally switched to use parameterized signals. The parameterized signal split at every coupler to form new parameterized signals, which can be monitored on spectrum analyzers to estimate optical crosstalk, or presented as a text list of all signals, including frequencies and powers for further analysis using analytical crosstalk estimates for multipath propagation. Fig. 18 shows the output at one fiber of an AWGM demultiplexer. Note the large number of PS (arrows) caused by the large number of crosstalk paths in the network. Also, the wavelength converters generate MFB signals. This example shows how the performance of a device in a subsystem can potentially affect a large network.

F. Interaction of Solitons in Nonlinear Dispersive Fibers (MFB versus SFB)

Solitons at two different wavelengths will walk through each other as they propagate along a dispersive fiber, because of their different group velocities. As they pass through each other, they will modulate each others' phases, via the nonlinear index of the fiber, whose slowly varying term depends on the sum of the powers in both waves. This process will cause frequency shifts in the pulses.

Soliton interaction can be modeled in two ways in PTDS as follows:

- by using the split-step Fourier method of *Fiber_NLS* acting on the combined fields of the two pulses within an SFB;
- by using the frequency-decomposition method in *FiberNLS_FD* acting on individual fields represented in MFB's. This method generally is much more numerically efficient.

Fig. 19 shows the spectrum of a 2-mW 300-ps pulse calculated using the two methods, when a 20-mW pulse walks through it in a dispersive nonlinear fiber. Both spectra are dynamically broadened by cross-phase modulation, and the agreement between the two methods is excellent. The saving is computation by using the frequency-decomposition method is a factor of 21.

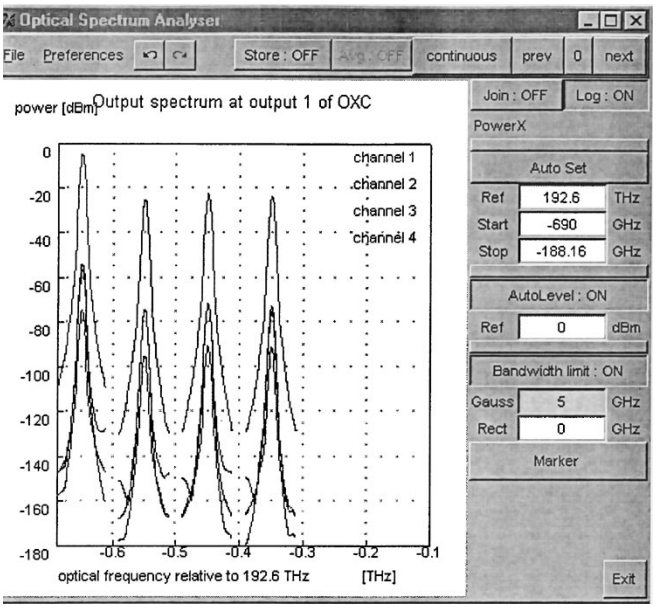

Fig. 16. Spectra of all of the outputs of the top AWGM of the optical cross connect simulated using MFB signals. Each channel represents one output of the AWGM.

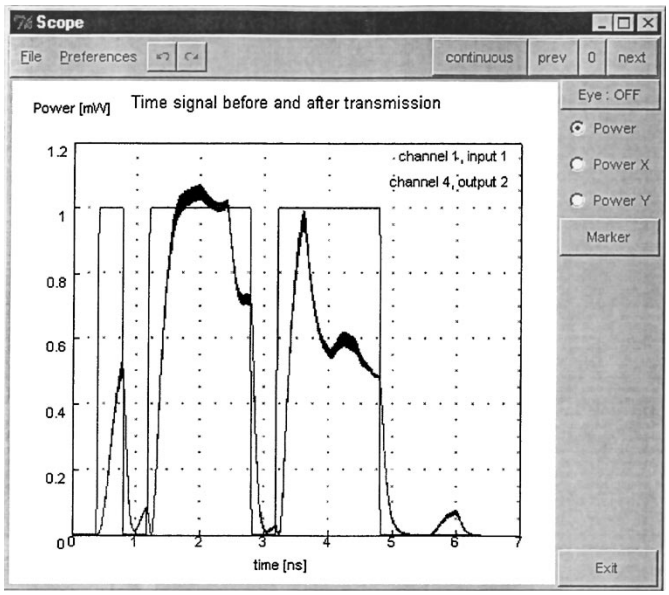

Fig. 17. Waveform of one switched and wavelength-converted channel (from top fiber WDM channel 1 to bottom fiber WDM channel 4) showing slow-leading edges and large fluctuations caused by crosstalk.

V. Conclusion

We have developed a flexible framework for photonic devices, systems, and networks simulation, together with a wide range of numerical modules representing photonic devices and subsystems. The multiple signal representations allow simulation at the optimum abstraction level for a problem. This simulation allows a design to be "roughed-out" using abstract signal representations, and then simulated thoroughly using detailed signal representations. The problem can also be partitioned spectrally, with abstract signal representations for noise and channels of little interest, or partitioned spatially, with subsystems being represented in more detail than the remainder of the network. We believe that our multirepresentation approach offers a future-proof platform for physical layer photonic device, system, and network simulations.

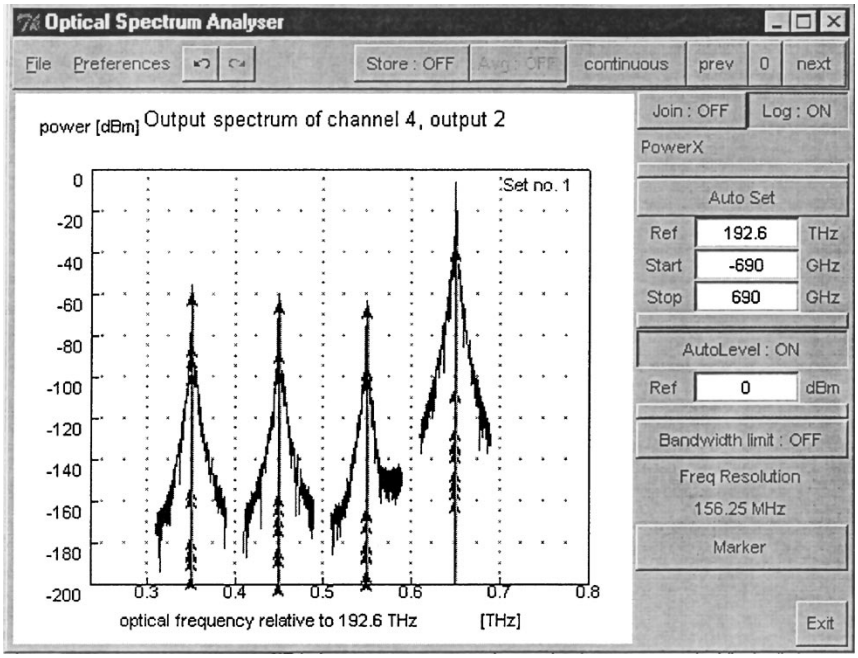

Fig. 18. Cross-connect simulation using parameterized signal inputs. The large number of parameterized signals (arrows) is caused by the large number of crosstalk paths in the network.

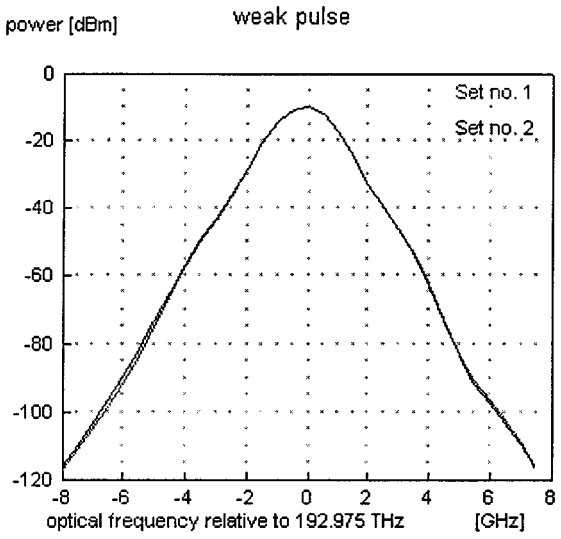

Fig. 19. Spectra calculated using (a) frequency decomposition and (b) split-step methods for a 2-mW pulse walking through a 20-mW pulse.

ACKNOWLEDGMENT

The authors would like to thank their development team, customers, university partners, and Scientific Advisory Board for help in steering the development of the multirepresentation simulation concept.

REFERENCES

[1] *J. Lightwave Technol.*, May 1988, vol. 6, Special Issue on Factors Affecting Data Transmission Quality.
[2] A. E. Willner, "Mining the optical bandwidth for a terabit per second," *IEEE Spectrum*, vol. 32, pp. 32–41, Apr. 1997.
[3] *IEEE J. Quantum Electron.*, Nov. 1998, vol. 34, Feature Issue on Fundamental Challenges in Ultrahigh-capacity Optical Fiber Communications Systems, pp. 2053–2103.
[4] T. Ono, "Approaching 1 bit/s/Hz spectral efficiency," in *Tech. Digest OFC'99*, San Diego, CA, Feb. 23–26, 1999, Paper FE4, pp. 410–411.
[5] A. Djupsjöbacka, "Prechirped duobinary modulation," *IEEE Photon. Technol. Lett.*, vol. 10, pp. 1159–1161, Aug. 1998.
[6] G. H. Smith, D. Novak, and A. Ahmed, "Technique for optical SSB generation to overcome dispersion penalties in fiber-radio systems," *Electron. Lett.*, vol. 33, pp. 74–75, 1997.
[7] Y. Shen, K. Lu, and W. Gu, "Coherent and incoherent crosstalk in WDM optical networks," *J. Lightwave Technol.*, vol. 17, pp. 759–764, May 1999.
[8] C. X. Yu, W.-K. Wang, and S. D. Brorson, "System degradation due to multipath coherent crosstalk in WDM network nodes," *J. Lightwave Technol.*, vol. 16, pp. 1380–1386, Aug. 1998.
[9] J. Nagal, "Dynamic behavior of amplified systems," in *Tech. Dig. OFC'99*, San Diego, CA, Feb. 23–26, 1999, Paper Th03, pp. 319–320.
[10] M. F. Mendez and M. A. Ali, "Simulation of 64 × 2.5 Gbit/s WDM transmission over 1056 km standard single-mode fiber using gain-flattened silica-based EDFAs," *IEEE Photon. Technol. Lett.*, vol. 10, pp. 300–302, Feb. 1998.
[11] H. Hamster and J. Lam, "PDA: Challenges for an emerging industry," in *Lightwave*. New York: Penwell, Aug. 1998.
[12] PTDS. Virtual Photonics Inc., Berlin, Germany. [Online]. Available: www.virtualphotonics.com.
[13] A. J. Lowery and P. C. R. Gurney, "Two simulators for photonic computer-aided design," *Appl. Opt.*, vol. 37, pp. 6066–6077, Sept. 1998.
[14] A. J. Lowery, "Computer-aided photonics design," *IEEE Spectrum*, vol. 34, pp. 26–31, Apr. 1997.
[15] Ptolemy simulation environment. University of California, Berkeley. [Online]. Available: www.ptolemy.eecs.berkeley.edu
[16] J. K. Ousterhout, *An Introduction to TCL and TK*. Redwood City, CA: Addison-Wesley, 1994.
[17] A. J. Lowery, P. C. R. Gurney, X.-H. Wang, L. V. T. Nguyen, Y.-C. Chan, and M. Premaratne, "Time-domain simulation of photonic devices, circuits and systems," in *Tech. Digest Phys. and Simul. Optoelectron. Devices IV*, vol. 2693, San Jose, CA, Jan. 29–Feb. 2 1996, pp. 624–635.
[18] C. J. Anderson and J. A. Lyle, "Technique for evaluating system performance using *Q* in numerical simulation exhibiting intersymbol interference," *Electron. Lett.*, vol. 30, pp. 71–72, 1994.
[19] G. Jacobsen, K. Bertilsson, and Z. Xiapin, "WDM transmission system performance: Influence of non-Gaussian detected ASE noise and periodic DEMUX characteristic," *J. Lightwave Technol.*, vol. 16, pp. 1804–1812, Oct. 1998.
[20] I. Kaminow and T. Koch, *Optical Fiber Telecommunications III*. New York: Academic, 1997.

[21] A. J. Lowery, A. Keating, and C. N. Murtonen, "Modeling the static and dynamic behavior of quarter-wave-shifted DFB lasers," *IEEE J. Quantum Electron.*, vol. 28, pp. 1874–1883, Sept. 1992.
[22] G. P. Agrawal, *Nonlinear Fiber Optics*. New York: Academic, 1995.
[23] R. Hui, M. O'Sullivan, A. Robinson, and M. Taylor, "Modulation instability and its impact in multispan optical amplified IMDD systems: Theory and experiments," *J. Lightwave Technol.*, vol. 15, pp. 1071–1082, 1997.
[24] D. Marcuse, C. R. Menyuk, and P. K. A. Wai, "Application of Manakov-PMD equation to studies of signal propagation in optical fibers with randomly varying birefringence," *J. Lightwave Technol.*, vol. 15, pp. 1735–1745, Sept. 1997.
[25] C. Caspar, H.-M. Foisel, A. Gladisch, N. Hanik, F. Kuppers, R. Ludwig, A. Mattheus, W. Pieper, B. Streubel, and H. G. Weber, "RZ versus NRZ modulation format for dispersion compensated SMF-based 10-Gb/s transmission with more than 100-km amplfier spacing," *IEEE Photon. Technol. Lett.*, vol. 11, pp. 481–483, Apr. 1999.
[26] V. S. Grigoryan and C. R. Menyuk, "A new linearization approach for modeling timing and amplitude jitter in dispersion-managed optical fiber communications," in *Tech. Digest OFC'99*, San Diego, CA, Feb. 23–26, 1999, Paper WM34, pp. 295–297.
[27] A. Richter and V. S. Grigoryan, "Efficient approach to estimate collision-induced timing jitter in dispersion-managed WDM RZ systems," in *Techn. Digest OFC'99*, San Diego, CA, Feb. 23–26, 1999, Paper WM33, pp. 292–294.
[28] J. Burgmeier, A. Cords, R. Marz, C. Schaffer, and B. Strummer, "A black-box model of EDFA's in WDM systems," *J. Lightwave Technol.*, vol. 16, pp. 1271–1275, July 1998.
[29] C. R. Giles and E. Desurvire, "Modeling erbium doped fiber amplifiers," *J. Lightwave Technol.*, vol. 9, pp. 271–283, Feb. 1991.
[30] A. Bononi and L. A. Rush, "Doped-fiber amplifier dynamics: A system perspective," *J. Lightwave Technol.*, vol. 16, pp. 945–956, 1998.
[31] M. J. Adams, H. J. Westlake, M. J. O'Mahoney, and I. D. Henning, "A comparison of active and passive bistability in semiconductors," *IEEE J. Quantum Electron.*, vol. QE-21, pp. 1498–1501, Sept. 1985.
[32] A. J. Lowery, "New inline wideband dynamic semiconductor laser amplifier model," *Proc. Inst. Elect. Eng.*, vol. 135, pp. 242–250, June 1988.
[33] M. M. Garcia and D. Uttamchanani, "Influence of the dynamic response of the Fabry–Perot filter on the performance of an OFDM-DD network," *J. Lightwave Technol.*, vol. 15, pp. 1778–1783, Aug. 1997.
[34] *J. Lightwave Technol.*, Aug. 1997, vol. 15, Special Issue on Fiber Gratings, Photosensitivity and Poling.
[35] D. Breuer and K. Petermann, "System modeling of high bit rate TDM- and WDM-systems," in *Integrated Photonics Research*, Santa Barbara, July 1999.
[36] R. Damle, R. Freund, and D. Breuer, "Outside-in evaluation of commercial WDM systems," in *Proc. Fiber Opt. Eng. Conf. (NFOEC)*, FL, 1999.
[37] C. Caspar, R. Freund, N. Hanik, L. Molle, and C. Peucheret, "Using normalized sections for the design of all optical networks," in *Proc. Opt. Network Design Model. Conf. (ONDM'2000)*, Athens, February 2000.
[38] E. L. Goldstein and L. Eskildsen, "Scaling limitations in transparent optical networks due to low-level crosstalk," *IEEE Photon. Tech. Lett.*, vol. 7, pp. 93–95, 1995.
[39] M. K. Smit and C. van Dam, "PHASAR-based WDM-devices: Principles, design and applications," *J. Selected Topics Quantum Electron.*, vol. 2, pp. 236–250, June 1996.

Arthur Lowery (M'92–SM'96), photograph and biography not available at the time of publication.

Olaf Lenzmann (S'96–A'98), photograph and biography not available at the time of publication.

Igor Koltchanov, photograph and biography not available at the time of publication.

Rudi Moosburger, photograph and biography not available at the time of publication.

Ronald Freund, photograph and biography not available at the time of publication.

André Richter, photograph and biography not available at the time of publication.

Stefan Georgi, photograph and biography not available at the time of publication.

Dirk Breuer, photograph and biography not available at the time of publication.

Herald Hamster, photograph and biography not available at the time of publication.